*Journal of Applied Electrochemistry* **33**: 1001–1009, 2003.



# Investigation of electroless plating of Ni–W–P alloy films

N. DU[1] and M. PRITZKER[2,*]
[1]*Department of Materials Science and Engineering, Nanchang Institute of Aeronautical Technology, Jiangxi, People's Republic of China*
[2]*Department of Chemical Engineering, University of Waterloo, Waterloo, Ontario, Canada N2L 3G1*
*(*author for correspondence, e-mail: pritzker@cape.uwaterloo.ca)*

Received 10 June 2002; accepted in revised form 3 June 2003

*Key words:* electroless, hypophosphite, nickel–tungsten–phosphorous alloy

**Abstract**

The electroless deposition of Ni–W–P alloy coatings onto metal substrates using $H_2PO_2^-$ as reducing agent from solutions containing nickel sulfate, sodium tungstate, sodium citrate, ammonium sulfate and other additives was studied. At most temperatures (60–80 °C) and pHs (7–11) investigated, bright and coherent coatings uniform in appearance were produced. Phosphorous and tungsten contents ranging from 3.5 to 8 wt % and 0.5 to 6 wt %, respectively, were obtained depending upon solution temperature and pH. Trends such as the effects of pH and temperature on average metal deposition rate and the P content in the alloy are similar to that reported previously for the Ni–P system. Correlation of open-circuit potentials with events occurring at the electrode surface in different solutions and polarization curves provide strong evidence that $Ni^{2+}$ ions participate in W and P deposition, $H_2$ evolution and $H_2PO_2^-$ oxidation and that $H_2PO_2^-$ ions participate in cathodic reduction. This indicates that the partial reactions for the Ni–W–P system do not occur independently of one another.

## 1. Introduction

Due to their corrosion and wear resistance, coating uniformity and ability to coat non-conductive surfaces, electroless nickel and nickel-based alloys are widely used in many industries. In the microelectronic, semiconductor and computer industries, they are used in printed circuits and magnetic record media [1]. A number of recent studies on electroless nickel plating have focused on novel applications in these industries [2–9]. With the miniaturization of integrated circuits by ultralarge-scale integration (ULSI) technology, attention has been focused on the replacement of aluminium with copper for the purposes of metallizing silicon substrates. Although copper has lower resistivity and enhanced electromigration resistance compared to aluminium, it suffers from some drawbacks such as poor corrosion resistance, poor adhesion to most dielectric materials and high diffusivity in silicon and silicon dioxide. However, such problems could be minimized through the application of a thin barrier layer between copper and the underlying substrate. Barriers based on the electroless deposition of such metals as Co, Ni and Ag using $H_2PO_2^-$ as a reducing agent have been investigated. It has been proposed that more reliable and superior diffusion barriers for copper interconnects can be obtained by incorporating tungsten into the films since Co–W–P and Ni–W–P alloys have greater hardness and melting points than Co–P and Ni–P alloys [10–12].

To date, little has been reported concerning the behaviour of the electroless plating of Ni–W–P ternary alloys. Accordingly, the objective of this study is to investigate the electroless plating of this system in further detail from baths containing nickel sulfate, sodium tungstate, sodium hypophosphite, sodium citrate, ammonium sulfate and minor amounts of other additives. The effects of bath temperature, pH and phosphite concentration on alloy composition and average deposition rate will be investigated and comparisons made with the known behaviour of the electroless plating of Ni–P alloys. Polarization curves for the Ni–W–P system will also be obtained to gain further insight into the interactions between the various components of the plating baths. The electroless reduction of nickel is always accompanied by the evolution of hydrogen gas. We will also focus attention on hydrogen evolution during Ni–W–P deposition and examine the effect of substrate on this reaction. These results will be discussed in relation to previously reported mechanisms for related alloy systems such as Ni–P and Co–W–P.

## 2. Experimental details

The solutions were prepared with reagent grade chemicals (Aldrich Chemical Company) and deionized water. All plating bath solutions used in this study contained the components at the compositions listed in Table 1. The effect of phosphite concentration in the plating bath was also investigated through the addition of phosphorous acid ($H_3PO_3$). Alloys were electrolessly plated onto three different metal substrates: rectangular coupons of copper (5 cm × 1 cm), mild steel (5 cm × 2 cm) and aluminium (5 cm × 1 cm), unless otherwise mentioned. The copper surface was contacted with an aluminium strip at the start of each experiment to be activated and to initiate plating.

The pretreatment of the substrates prior to plating involved the following sequence of steps: polishing with SiC abrasive paper (600 grade), cleaning with a detergent, rinsing with deionized water, ultrasonic cleaning for 30 min while immersed in deionized water, another rinsing with deionized water, drying with acetone before storage in a desiccator. Prior to plating, each specimen was etched in a 20 wt % sulfuric acid solution for 3 min and then transferred to a 5 wt % sulfuric acid solution for 5 min to activate its surface. This was followed by a rinse with deionized water, drying with acetone and weighing before immersion into the plating bath.

Plating experiments were conducted by immersing the substrates into 300 ml plating solution and carrying out deposition for 60 min. Typically, a coating with a mass of at least 20 mg was produced over this period. No external agitation of the solution was provided, although the evolution of $H_2$ during deposition ensured some degree of mixing. The pH during plating was varied from 7 to 11 through the addition of $NH_4OH$. The solution temperature was controlled by immersing the plating cell in a controlled water bath. Experiments were carried out at temperatures between 60 and 85 °C (±2 °C). Following electroless plating, each sample was dried and then reweighed. From the mass change, the average deposition rate over the substrate area and over the plating time was determined. After being weighed, the specimen was set aside for elemental analysis.

The composition of each Ni–W–P alloy was determined by completely dissolving the coating and then analysing the resulting solution for its nickel, tungsten and phosphorous content using direct current plasma (DCP) spectroscopy. The complete dissolution of the alloy deposit was ensured by immersing the coating in an acidic solution containing 3 parts HCl and 1 part $HNO_3$ for 10 min.

A series of experiments was also conducted to determine the volume of hydrogen gas evolved during the deposition process. For this purpose, plating experiments were carried out in a cell sealed except for a vent connected to an inverted graduated cylinder initially filled with water. As gas evolved from the substrate, it was vented off and collected in the cylinder and its volume measured from the amount of water displaced in the cylinder.

The data on alloy composition, deposition rates, $H_2$ evolution volume and open-circuit potentials presented in this paper represent the average of at least three measurements. The variability of each of these measurements was found to be well within 10% in all cases.

Ni–W–P alloy deposition kinetics were studied by carrying out linear potential scans at 10 mV $s^{-1}$ using an Eco Chemie PGSTAT 30 Autolab potentiostat/galvanostat. A three-electrode system involving a copper disc working electrode (exposed area 0.28 $cm^2$), platinum wire counter electrode and saturated calomel reference electrode was used for this purpose. The working electrode was mounted to the end of a Teflon shaft of a rotating disc assembly (Pine Instruments). A rotational speed of 500 rpm was used in this study. All electrode potentials reported in this study correspond to the standard calomel scale.

*Table 1.* Composition of electroless plating bath used in this study

| | |
|---|---|
| Nickel sulfate ($NiSO_4 \cdot 6H_2O$) | 0.1 mol $L^{-1}$ |
| Sodium tungstate ($Na_2WO_4 \cdot 2H_2O$) | 0.2 mol $L^{-1}$ |
| Sodium hypophosphite ($NaH_2PO_2 \cdot H_2O$) | 0.2 mol $L^{-1}$ |
| Sodium citrate ($Na_3C_6H_5O_7 \cdot 2H_2O$) | 0.3 mol $L^{-1}$ |
| Ammonium sulfate ($(NH_4)_2SO_4$) | 0.2 mol $L^{-1}$ |
| Lactic acid ($CH_3CHOHCOOH$) | 5 mg $L^{-1}$ |
| Lead acetate ($Pb(CH_3CO_2)_2 \cdot 3H_2O$) | 2 mg $L^{-1}$ |

## 3. Results and discussion

### 3.1. *Effect of bath temperature and initial pH*

Under all experimental conditions reported in this Section, bright and coherent Ni–W–P alloy coatings uniform in appearance were obtained. The effect of bath temperature on the average alloy deposition rate and the tungsten and phosphorous content in the deposits formed on copper substrates is shown in Figure 1. These results were obtained at an initial pH 9.0 in a solution with composition given in Table 1. Although the added sodium citrate provided buffering capability, the pH

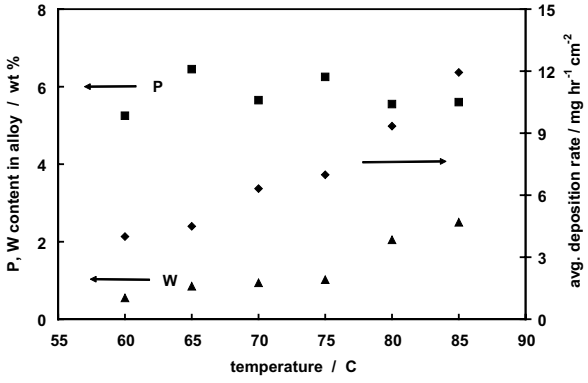


*Fig. 1.* Effect of temperature on (■) wt % P and (▲) wt % W in the alloys and (♦) average metal deposition rate resulting from electroless plating onto copper substrates in the base solution (Table 1) at initial pH 9.0.

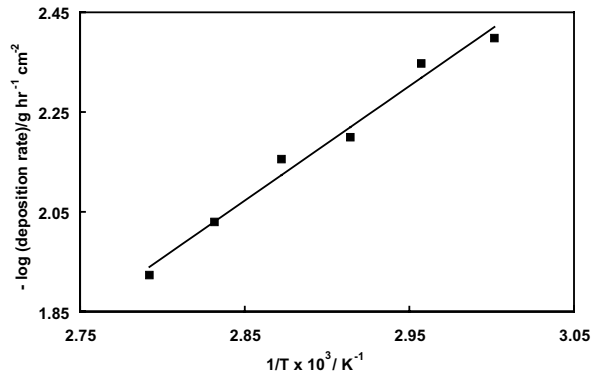


*Fig. 2.* Arrhenius plot of average metal deposition rate resulting from electroless plating in the base solution (Table 1) at initial pH 9.0.

nevertheless decreased (as much as 0.5 pH unit) over the course of each plating experiment. A similar trend has been observed during Ni–P alloy plating [1]. With an increase of temperature from 60 to 85 °C, the average deposition rate increases from about 4 to 12 mg $h^{-1}$ $cm^{-2}$. Over the same range, the phosphorus content remains approximately constant between 5 and 6.5 wt %. These levels are comparable to those reported in Ni–P alloys at similar pH and solution conditions [1, 13, 14]. The tungsten content remains constant below 1 wt % under 75 °C and then rises to about 2.5 wt % at 85 °C. Apparently, the presence of 0.2 mol $L^{-1}$ tungstate in the solution and the plating of tungsten do not significantly affect the plating behaviour of the other components.

An Arrhenius plot for the temperature dependence of the average alloy deposition rate at initial pH 9.0 is presented in Figure 2. The data follow linear behaviour from 60 to 85 °C, yielding an activation energy of 43.98 kJ $mol^{-1}$. This value is comparable to those reported for the deposition of Ni–P alloys in similar type solutions [1].

The effects of initial solution pH at 80 °C on the average deposition rate onto copper substrates and the resulting W and P contents are shown in Figure 3. An increase in initial pH from 7.0 to 11.0 tends to lower the W and P content, similar to trends reported for P in Ni–P alloys [1, 13–15]. This is also consistent with findings of Ebn Touhami et al. [16] from polarization experiments that an increase in pH from 9 to 10.5 enhances $Ni^{2+}$ reduction and $H_2PO_2^-$ oxidation kinetics, but does not affect $H_2PO_2^-$ reduction to P. As shown in Figure 3, the average deposition rate increases to a maximum at pH 9.0, although the effect is not large. Abrantes and Correia [13] reported similar behaviour for the Ni–P system. Ebn Touhami et al. [16] also showed from electrochemical impedance spectroscopy that charge transfer resistance for Ni–P deposition is a minimum at pH 9.0.

### 3.2. *Effect of phosphite concentration*

The effect of phosphite ions was determined from a series of experiments in which varying amounts of $H_3PO_3$ were added to the base solution described in Table 1 at pH 9.0 and 80 °C. Since phosphite is produced during electroless plating, one might expect its presence to have some effect on the process, particularly as its concentration builds up. However, as shown in Figure 4, the addition of as much as 2.4 mol $L^{-1}$ phosphite has little effect on alloy composition or the average deposition rate. In addition, it does not adversely affect deposit quality that remains excellent or plating bath stability during usage or storage. A given bath could be used for up to eight consecutive plating runs without any harmful effects with only nickel sulphate and sodium hypophosphite being added to compensate for deposited metal. It should be noted that the $H_3PO_3$ concentrations added in these experiments (Figure 4) are much higher than any amount produced during plating by $H_2PO_2^-$ oxidation. Thus, phosphite build-up during plating should not limit the bath lifetime in a commercial operation.

### 3.3. *Effect of substrate*

The average deposition rates and the volume of $H_2$ generated (corresponding to conditions of 80 °C and

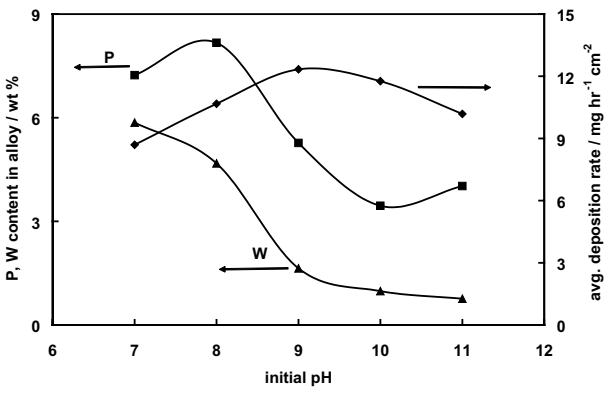


*Fig. 3.* Effect of initial pH on (■) wt % P and (▲) wt % W in the alloys and (♦) average metal deposition rate resulting from electroless plating in the base solution (Table 1) at 80 °C.

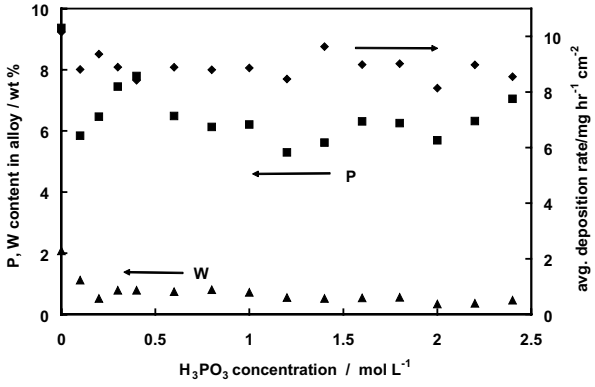


*Fig. 4.* Effect of $H_3PO_3$ concentration on (■) wt % P and (▲) wt % W in the alloys and (♦) average metal deposition rate resulting from electroless plating in the base solution (Table 1) at 80 °C and initial pH 9.0.

1 atm) during electroless plating of Ni–W–P alloys at initial pH 9.0 and 80 °C were measured and compared for copper, mild steel and aluminium substrates. On first contact of the mild steel and aluminium surfaces with the solution, somewhat unsteady open-circuit potentials in the range of −0.92 and −1.10 V, respectively, were observed. As the alloy coating began to accumulate, the open-circuit potential stabilized and levelled off at −0.89 V thereafter. The copper substrate exhibited very different behaviour. Upon immersion in the solution, it remained electroinactive and exhibited an open-circuit potential of −0.55 V, well above that measured on the other substrates. However, the copper was immediately activated by contacting an aluminium strip, lowering the open-circuit potential to the level characteristic of the aluminium substrates and allowing deposition and $H_2$ evolution to commence. Similar behaviour has been noted by Abrantes and Correia [13] for the Ni–P system.

Analysis of the alloys produced showed that the nature of the substrate has little effect on the average deposition rate except during the first few minutes of plating. A comparison of the volume of hydrogen evolved during Ni–W–P alloy deposition on the copper, mild steel and aluminium surfaces is shown in Figure 5. The amount of hydrogen produced varies with substrate in the following order: copper < mild steel < aluminium. Examination of the curves in Figure 5 shows that the gas evolution rate is highest in the first few minutes of plating and then slows down to a largely constant value during the remainder of the process. The open-circuit potentials on the mild steel and pure aluminium substrates measured at the start of electroless plating are more negative than that on the nickel surfaces produced during plating. Since a more negative potential should allow more hydrogen to be produced, one would expect a higher rate of gas evolution at the outset of plating followed by a gradual decline as the surface becomes more nickel-like. Furthermore, the difference in the amount of gas evolved on the three substrates is established in the first few minutes and is largely unchanged thereafter.

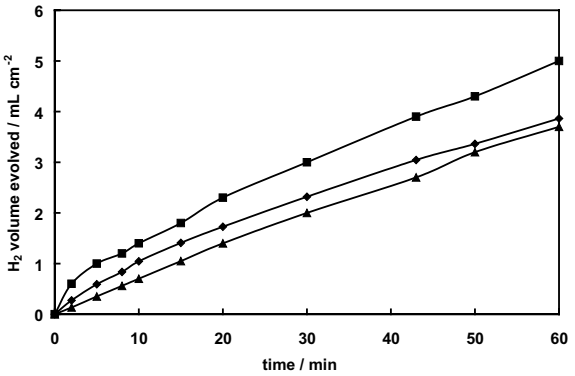


*Fig. 5.* Volume of $H_2$ evolved over the course of electroless plating in the base solution (Table 1) at 80 °C and initial pH 9.0 on (■) aluminium, (♦) mild steel and (▲) copper substrates. $H_2$ volumes are reported for conditions of 80 °C and 1 atm.

### 3.4. *Measurement of molar ratios of reaction products*

In view of the results presented so far, the mechanism for the Ni–W–P system should be similar to those proposed for related alloys systems such as Ni–P and Co–W–P [1, 12, 13, 15–18]. Although these mechanisms differ in some regards, most incorporate the following features: (i) produced $H_2$ originates primarily from the hypophosphite reducing agent rather than $H_2O$ [19, 20] and (ii) oxidation and reduction reactions mediated by radicals play very important roles in addition to anodic and cathodic processes involving direct electron transfer. These characteristics ensure that metal deposition is always accompanied by $H_2$ evolution. With this in mind, one might expect the predominant overall reactions during Ni–W–P electroless plating in an alkaline solution to be the following:

$$Ni^{2+} + 2\,H_2PO_2^- + 2\,OH^- \rightarrow Ni^0 + 2\,H_2PO_3^- + H_2 \quad (1)$$

$$WO_4^{2-} + 6\,H_2PO_2^- + 4\,H_2O \rightarrow W^0 + 6\,H_2PO_3^- + 3\,H_2 + 2\,OH^- \quad (2)$$

$$2\,H_2PO_2^- \rightarrow P^0 + 1/2\,H_2 + H_2PO_3^- + OH^- \quad (3)$$

$$H_2PO_2^- + H_2O \rightarrow H_2 + H_2PO_3^- \quad (4)$$

These reactions reflect the overall stoichiometry of the processes, but not the possible mechanistic steps or interactions between the various reactants.

The molar ratios of the products generated on copper substrates during our electroless plating experiments have been obtained and compared to the stoichiometry of Reactions 1–4. Table 2 shows the ratio of the number of moles of $H_2$ generated to the number of $H_2$ moles expected from Reactions 1–3 on the basis of the number of moles of Ni, P and W produced at 80 °C and various initial pH. Also included is the ratio of the number of moles of $H_2$ generated to the number of Ni deposited. Both ratios should exceed 1.0 if electroless plating proceeds via Reactions 1–4 exclusively. As shown, both ratios exceed 1.0 at pH 7 and 10, but fall below 1.0 at pH 8 and 9. This indicates that Reactions 1–4 do not

*Table 2.* Molar ratios of products generated during metal deposition on copper substrates at 80 °C

| pH | $\frac{n_{H_2}(\text{meas})}{n_{H_2}(\text{pred})}$ | $\frac{n_{H_2}(\text{meas})}{n_{Ni}(\text{meas})}$ |
|---|---|---|
| 7 | 1.23 | 1.41 |
| 8 | 0.85 | 0.96 |
| 9 | 0.87 | 0.93 |
| 10 | 1.05 | 1.10 |

Note: $n_{H_2}(\text{meas})$ and $n_{Ni}(\text{meas})$ correspond to the number of moles of $H_2$ and Ni, respectively, generated during electroless deposition; $n_{H_2}(\text{pred})$ corresponds to the number of moles of $H_2$ predicted on the basis of the stoichiometry of Reactions 1–3 and the amounts of Ni, W and P deposited during electroless plating.

completely describe the plating process. Specifically, reactions that produce less $H_2$ or that consume $H_2$ must also occur, particularly at pH 8 and 9. Petrov et al. [18] found evidence that some $WO_4^{2-}$ is reduced to $WO_2$ rather than to W during the formation of Co–W–P alloys. There are also indications from the work of Genutiene et al. [21] on the electroless deposition of Ni–Re–P alloys that hydrogen atoms or radicals formed as intermediates during $H_2PO_2^-$ oxidation (i.e., Reaction 4) participate to some extent in the reduction of $ReO_4^-$ to Re. The reduction of $WO_4^{2-}$ may proceed similarly to that of $ReO_4^-$. Also, several groups have formulated partial reactions in which P is produced without the production of $H_2$ [13, 15, 16, 18]. Although it is quite likely that these reactions involving tungsten and phosphorous occur, they cannot completely account for the discrepancy with the measured amount of $H_2$ at pH 8 and 9 due to the small amounts of W and P deposited. More importantly, since fewer moles of $H_2$ than Ni are being produced at these pH, Reaction 1 cannot provide the correct overall stoichiometry for $Ni^{2+}$ reduction. The observed molar ratios are possible if nickel deposition and hydrogen evolution are viewed as being parallel reactions in which reduction occurs through the mediation of adsorbed radicals, [13, 15, 16]. For example,

$$2\,\dot{H}(ads) + Ni^{2+} \rightarrow 2\,H^+ + Ni^0$$

$$2\,\dot{H}(ads) \rightarrow H_2$$

or direct electron transfer

$$Ni^{2+} + 2\,e^- \rightarrow Ni^0$$

$$2\,H^+ + 2\,e^- \rightarrow H_2$$

For both pathways, a rise in pH favours Ni deposition over $H_2$ evolution, in agreement with the trend in the $n_{H_2}/n_{Ni}$ ratios from pH 7 to 9 shown in Table 2. This also is consistent with the effect of initial pH on metal deposition rate shown in Figure 3 and also reported previously by Abrantes and Correia [13] and Ebn Touhami et al. [16].

In all of these cases, the $n_{H_2}/n_{Ni}$ ratios increase and the metal deposition rates decrease as the pH is increased above 9 since electroless plating was conducted in ammoniacal solutions. As discussed by Abrantes and Correia [13], a rise in pH favours conversion of $NH_4^+$ to $NH_3$ and aqueous nickel amine complexes. It is likely that the discharge of these complexes does not occur as readily as discharge of bare $Ni^{2+}$ ions.

### 3.5. *Open-circuit potentials of alloy surface in different solutions*

To further study the relation between the various reactions and electroless deposition, we conducted the following experiment. A Ni–W–P coating was electrolessly deposited onto a copper coupon for 15 min in a bath with the composition given in Table 1 at pH 9.0 and temperature of 80 °C. The coupon was then transferred to another solution at the same temperature, pH and composition, except with nickel sulphate absent. The open-circuit potential of the coupon in this second solution was then monitored and any visible changes within the cell were noted. This procedure was repeated on another fresh copper substrate, but now with a different second solution containing 0.1 mol $L^{-1}$ nickel sulphate and all the other components listed in Table 1 except sodium hypophosphite.

A comparison of the open-circuit potentials of the two coupons immersed in the different second solutions is shown in Figure 6. When $H_2PO_2^-$ is absent from the second solution, there is no sign of $H_2$ evolution or metal deposition during the 50 min immersion time. When first exposed to this solution, the coupon displays an open-circuit potential of about −0.60 V vs SCE that gradually increases to about −0.50 V SCE by the end of the experiment. These potentials are well above the open-circuit potentials of about −0.89 V vs SCE measured in the presence of $H_2PO_2^-$.

A considerably different electrode response is obtained when the coupon is immersed in the second solution in which only nickel sulfate is absent. A more negative open-circuit potential of −0.945 V is initially measured and slowly changes to about −0.90 V by the end of 22 min. As noted above, these potentials are close to those observed during electroless plating. Over this time, a considerable amount of $H_2$ is generated on the coupon surface. However, from measurement of the coupon mass and visual examination of its surface, there is no evidence of deposition of W or P. The electroless plating of W and P apparently requires the addition of $Ni^{2+}$ as well as that of $H_2PO_2^-$ ions in solution. Although the measured open-circuit potentials between −0.945 and −0.9 V are negative enough for W and P deposition, this obviously is not the only requirement.

The difficulty in plating tungsten and phosphorous in single metal systems has been noted for some time

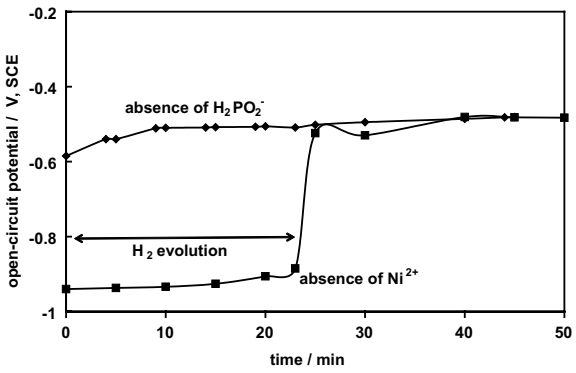


*Fig. 6.* Open-circuit potentials of a Ni–W–P alloy-coated copper substrate immersed in the base solution (Table 1) at 80 °C and initial pH 9.0 with (■) nickel sulphate removed and (♦) sodium hypophosphite removed.

[22–24]. The enhancement in the incorporation of P in the alloys due to the presence of nickel is consistent with the polarization results of Ebn Touhami et al. [16]. This may be due to an interaction between the metals in their aqueous forms [16] or through the action of radicals formed by the spontaneous adsorption and homolysis of $H_2PO_2^-$ catalysed by the nickel surface [13, 25]. Another possibility is induced co-deposition proposed to explain why refractory metals such as Mo or W cannot be plated electrolytically in single metal systems, but can be easily deposited in alloys with iron-group metals [24, 26]. Whether one or more of these interactions occurs, the reduction reactions apparently do not occur independently of each other. A similar conclusion was reached by Abrantes and Correia [13] regarding the Ni–P system.

The open-circuit potentials between −0.945 and −0.9 V measured over the first 22 min in the absence of $Ni^{2+}$ while $H_2$ is being formed are much closer to those observed during electroless plating than to those measured in the absence of $H_2PO_2^-$ (Figure 6). This suggests that $H_2PO_2^-$ oxidation controls the overall process, similar to that reported for the Ni–P [15,27] and Co–W–P [11, 18] systems.

After about 22 min in the second solution, $H_2$ evolution abruptly ceases and the open-circuit potential simultaneously rises rapidly to −0.554 V, closely coinciding with that observed in the solution containing no $H_2PO_2^-$. For the remainder of the experiment, no $H_2$ formation is evident and the open-circuit potential closely traces the response obtained in the absence of the reducing agent. Presumably, some type of passivation of the previously formed Ni–W–P surface has occurred and the conditions for $H_2$ evolution no longer exist [16, 27, 28]. Thus, the presence of $H_2PO_2^-$ does not guarantee that $H_2$ will be formed and that the condition of the substrate is also important.

### 3.6. *Polarization experiments in complete plating bath*

A series of polarization curves was obtained for the Ni–W–P system in complete plating baths (Table 1) for temperatures ranging from 60 to 80 °C at pH 9.0. Each experiment involved first pre-coating a copper rotating disc with the alloy by electroless plating from a complete plating bath at the desired temperature. This was followed by polarization of the coated disc by linear sweep voltammetry in the same solution. Each scan began at the negative-most potential and proceeded in the positive direction at a rate of 10 mV $s^{-1}$. The disc was rotated at a speed of 500 rpm throughout both the coating and polarization stages.

The resulting voltammograms obtained at 60 and 80 °C are presented in Figure 7. The voltammograms at the other temperatures are very similar and so have not been included here. The electrode responses are unaffected whether or not the solution is deoxygenated or the disc is electrolessly pre-coated with a Ni–W–P alloy prior to the voltammetric scan.

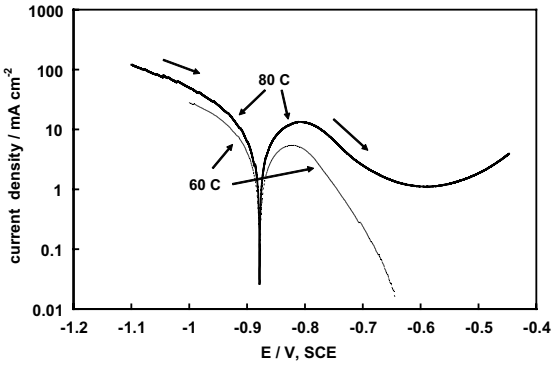


*Fig. 7.* Polarization curves obtained from linear potential scans of alloy-coated copper electrodes immersed in the base solution (Table 1) at 60 °C and 80 °C and pH 9.0. The scans were carried out at 10 mV $s^{-1}$ from −1.0 to −0.64 V SCE at 60 °C and from −1.1 to −0.45 V SCE at 80 °C.

Each voltammetric scan in Figure 7 is characterized by a sharp drop in cathodic current at about −0.89 V, followed by an equally sharp rise in anodic current. At the start of each scan, cathodic reduction of the metal ions and evolution of $H_2$ occur on the substrate surface at a substantial rate. However, as shown elsewhere [15, 25, 27], the $H_2PO_2^-$ oxidation catalysed by the growing Ni-dominated alloy surface can also occur along the cathodic branch at reductant concentrations above 0.1 mol $L^{-1}$. It has previously been shown that the initial current rise along the anodic branch involves $H_2PO_2^-$ oxidation rather than the oxidation of deposited metal [15, 17, 25, 29]. Thus, at −0.89 V, a balance likely exists between the cathodic current due to metal reduction and hydrogen evolution and the anodic current due to $H_2PO_2^-$ oxidation. With a further increase in potential above −0.89 V, $H_2PO_2^-$ oxidation begins to dominate, causing a sharp rise in anodic current.

Comparison of the open-circuit potential $E_p$ measured during electroless plating and the electrode potential $E_{oc}$ at which the current of the anodic and cathodic branches on the polarization curves simultaneously drop to zero is shown in Table 3 at the various temperatures. In each case, there is good agreement between $E_p$ and $E_{oc}$.

Another point can be made concerning the anodic branches of the polarization curves in Figure 7. After the initial current rise above −0.89 V, it begins to decrease significantly as the potential reaches approximately −0.85 V. Similar behaviour observed in polarization curves for the Ni–P system has been ascribed to passivation of the electrode surface [16, 27, 28]. It is noteworthy that the potentials where this passivation is observed in the polarization curves agrees well with where the abrupt rise in open-circuit potentials occurs when the alloy coating is immersed in a $Ni^{2+}$-free solution (Figure 6). This abrupt change in open-circuit potential coincides with the cessation of $H_2$ evolution and any apparent electrode activity, as would be expected if the surface becomes passivated.

*Table 3*. Comparison of open-circuit potentials measured during electroless plating with those obtained from polarization curves at pH 9.0

| Temperature /°C | $E_p^*$ vs SCE/V | $E_{oc}^\dagger$ vs SCE/V |
|---|---|---|
| 60 | −0.863 | −0.879 |
| 65 | −0.875 | −0.886 |
| 70 | −0.878 | −0.882 |
| 75 | −0.883 | −0.882 |
| 80 | −0.885 | −0.882 |

* obtained from direct measurement during electroless plating.
† obtained from analysis of polarization curves.

### 3.7. *Polarization experiments in partial plating baths at 80 °C and pH 9.0*

Polarization curves were obtained in partial plating baths at 80 °C and pH 9.0 for comparison with the one in Figure 7 obtained in the complete plating bath. Once again, voltammetric scans were conducted at 10 mV $s^{-1}$ on alloy surfaces precoated by electroless plating from the base solution (Table 1) at 80 °C and pH 9.0. Figure 8 presents polarization curves for the alloy-coated electrodes in hypophosphite-less and complete plating solutions (the latter is taken from Figure 7 with current density plotted on a linear scale). The two curves display significant differences. Whereas the overall current changes from cathodic to anodic in the case of the complete plating bath as the electrode potential rises above about −0.89 V, it remains cathodic throughout the entire scan in the absence of $H_2PO_2^-$. Although not shown here, the current only becomes anodic when the scan is extended above −0.55 V. This potential agrees well with the open-circuit potentials shown in Figure 6 in the absence of $H_2PO_2^-$.

At very negative potentials, the current measured in the complete solution is higher than when $H_2PO_2^-$ is removed. A similar enhancement by $H_2PO_2^-$ of the cathodic processes has been observed in the Ni–P system

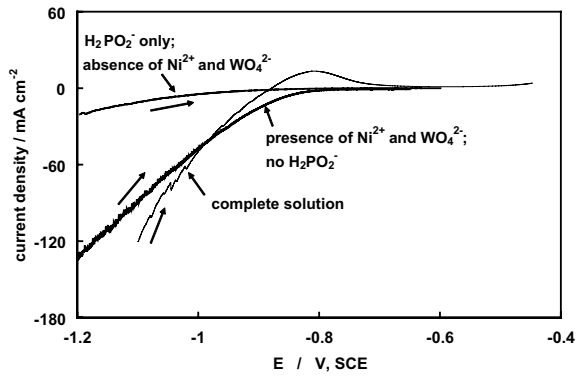


*Fig. 8*. Polarization curves obtained from potential scans of alloy-coated copper electrodes immersed in the following solutions at 80 °C and pH 9.0: base solution (Table 1), base solution with $NaH_2PO_2 \cdot H_2O$ absent and base solution with $NiSO_4 \cdot 6H_2O$ and $Na_2WO_4 \cdot 2H_2O$ absent.

from voltammetry experiments [15, 16] and EQCM measurements [30]. A cross-over in the curves occurs whereby the cathodic current in the presence of $H_2PO_2^-$ becomes less than that obtained in its absence when the potential exceeds −0.98 V. Given that the anodic peak above −0.89 V is associated with $H_2PO_2^-$ oxidation, this observation further supports the idea that $H_2PO_2^-$ oxidation occurs with metal reduction and $H_2$ evolution during cathodic polarization.

A voltammetric scan between −1.2 V and −0.6 V was obtained on an alloy-coated electrode immersed in the base solution with nickel sulphate and sodium tungstate removed. The resulting electrode response is also shown in Figure 8. The cathodic current at the negative end of the scan is associated with the reduction of the solvent. The voltammogram is marked by the current being cathodic everywhere except in a region between −0.72 and −0.66 V (although not obvious from the scale of the plot). Over this range, a small anodic current with a maximum of 0.05 mA $cm^{-2}$ is measured. Abrantes and Oliveira [17] presented voltammograms for nickel electrodes in hypophosphite solutions similar to those shown in Figure 8 and attributed the anodic current rise to $H_2PO_2^-$ oxidation. The magnitude of this current was strongly dependent on electrolyte composition. The addition of sodium citrate, also present in the solutions used in our study, tends to suppress $H_2PO_2^-$ oxidation current to levels observed in Figure 8.

Comparison of the electrode response obtained in the hypophosphite-only solution with the voltammogram obtained in the complete plating bath reveals that considerably more $H_2PO_2^-$ oxidation occurs in the presence of $Ni^{2+}$ ions. Also, the current rise for this process occurs at significantly more negative potentials when $Ni^{2+}$ ions are added. Thus, not only is the catalytic nature of the electrode surface important for $H_2PO_2^-$ oxidation, but so is the participation of $Ni^{2+}$ ions.

We conducted an experiment identical to that shown in Figure 8 in which 0.2 mol $L^{-1}$ sodium tungstate and 0.2 mol $L^{-1}$ sodium hypophosphite were added, but nickel sulfate was absent. Although not shown here, the resulting electrode response is very similar to that for the hypophosphite-only solution in Figure 8, indicating that the presence of tungstate does not affect the electrochemical behaviour of $H_2PO_2^-$.

Comparison of Figures 6 and 8 when the electrolyte is free of nickel and tungsten reveals differences in the electrode responses although the electrolyte compositions are identical. The results shown in Figure 6 indicate an open-circuit potential of −0.95 to −0.9 V, whereas the voltammogram in Figure 8 indicates that $H_2PO_2^-$ oxidation only begins when potential reaches about −0.72 V. The most obvious difference in the conditions in the two cases is that the solution was more intensely agitated during the rotating disc experiments shown in Figure 8. The positive shift in the electrode potentials during $H_2PO_2^-$ oxidation when the solution is more strongly agitated suggests that convection tends to suppress this process. This could be due to convection enhancing

passivation or dissolution of the electrode surface, removal of active intermediates of the oxidation process from the electrode surface [31] or transport of trace amounts of oxygen to the electrode surface where its subsequent reduction could interfere with $H_2PO_2^-$ oxidation.

### 3.8. *Applicability of Wagner–Traud mixed-potential theory*

According to Wagner–Traud mixed potential theory, the half-cell anodic and cathodic reactions occur independently of each other [32]. From open-circuit potential and polarization experiments for the Ni–W–P system in the previous sections, there is ample evidence of the interaction of $Ni^{2+}$ ions in P and W deposition and $H_2PO_2^-$ oxidation and the interaction of $H_2PO_2^-$ ions in cathodic reduction. Thus, Wagner–Traud theory does not appear to be applicable to the electroless plating of Ni–W–P alloys. Similar evidence has been presented for the Ni–P system by a number of other groups [13, 15, 16, 20, 28].

To further test the applicability of Wagner–Traud theory, we compare the polarization curves in Figure 8 obtained in the presence of nickel sulfate and sodium tungstate, but no $H_2PO_2^-$, with the scan obtained in the hypophosphite-only solution. There is no potential at which cathodic current on the metal-only curve and anodic current on the hypophosphite-only curve flow in equal amounts. In fact, close to the open-circuit potentials measured during electroless plating, only cathodic current is observed in both cases. Thus, the open-circuit potential observed during electroless plating cannot be predicted from the partial reaction polarization curves according to Wagner–Traud theory. Only the polarization curve such as Figure 7 obtained in a complete plating bath has been found to be applicable to the conditions of electroless plating.

## 4. Summary

Bright, coherent and uniform Ni–W–P alloy coatings have been produced on copper, aluminium and mild steel substrates from solutions containing nickel sulfate, sodium tungstate, sodium hypophosphite, sodium citrate, ammonium sulfate and small amounts of lactic acid and lead acetate. Some trends observed in Ni–W–P plating are similar to those previously reported for the Ni–P system. An increase in temperature from 60 to 85 °C at pH 9 raises the average metal deposition rate, while the P content in the resulting alloy remains between 5 and 6.5 wt %. Meanwhile, the W content in the alloy increases gradually from about 0.5 to 2.5 wt %. The general effect of pH on alloy composition has also been found to be similar to that reported previously for the Ni–P system, with the content of the minor components decreasing with a pH rise from 7 to 11. The presence of 0.2 mol $L^{-1}$ $Na_2WO_4 \cdot 2H_2O$ does not qualitatively affect the behaviour of the system.

Open-circuit potential measurements and polarization curves obtained in various solutions provide strong evidence for the direct participation of $Ni^{2+}$ ions in W and P deposition and $H_2PO_2^-$ oxidation and the participation of $H_2PO_2^-$ in cathodic reduction. From these results, Wagner-Traud mixed potential theory does not appear to apply to the electroless plating of Ni–W–P alloys and polarization curves obtained in the complete plating solution should be used to study this system.

## Acknowledgements

Gratitude is expressed to the China Scholarship Council for providing one of the authors (N. Du) with a fellowship to study abroad and to the Natural Sciences and Engineering Research Council of Canada (NSERC) for financial support during the project.

## References

1. G.O. Mallory and J.B. Hajdu, '*Electroless plating*: *Fundamentals and Applications*', (AESF, Orlando, FL, 1990).
2. Y. Okinaka and T. Osaka, *in* H. Gerischer and C.W. Tobias (Eds), '*Advances in Electrochemical Science and Engineering*', Vol. 3, (VCH, Weinheim/New York, 1994), p. 55.
3. N. Takano, N. Hosoda, T. Yamada and T. Osaka, *Electrochim. Acta* **44** (1999) 3743.
4. S. Zhang, J. De Baets, M. Vereeken, A. Vervaet and A. Van Calster, *J. Electrochem. Soc.* **146** (1999) 2870.
5. T. Osaka, T. Misato, J. Sato, H. Akiya, T. Homma, M. Kato, Y. Okinaka and O. Yoshioka, *J. Electrochem. Soc.* **147** (2000) 1059.
6. S.Z. Chu, M. Sakairi, H. Takahashi, K. Simamura and Y. Abe, *J. Electrochem. Soc.* **147** (2000) 2181.
7. T. Homma, Y. Kita and T. Osaka, *J. Electrochem. Soc.* **147** (2000) 4138.
8. M.C. Zhang, E.T. Kang, K.G. Neoh and K.L. Tan, *J. Electrochem. Soc.* **148** (2001) C71.
9. Á. Révész, J. Lendvai, J. Lóránth, J. Pádár and I. Bakonyi, *J. Electrochem. Soc.* **148** (2001) C715.
10. F.P. Perlstein, R.F. Weightman and R. Wick, *Met. Fin.* **61** (1963) 77.
11. Y.-S. Kim, S. Lopatin and Y. Shacham-Diamand, *in Proceedings of the 1997 IEEE/Cornell Conference on* '*Advanced Concepts in High Speed Semiconductor Devices and Circuits*', 4–6, Aug. 1997, Ithaca, NY (1997), pp. 192–200.
12. Y. Shacham-Diamand, Y. Sverdlov and N. Petrov, *J. Electrochem. Soc.* **148** (2001) C162.
13. L.M. Abrantes and J.P. Correia, *J. Electrochem. Soc.* **141** (1994) 2356.
14. Y.-S. Kim and H.-J. Sohn, *J. Electrochem. Soc.* **143** (1996) 505.
15. M. Ebn Touhami, M. Cherkaoui, A. Srhiri, A. Ben Bachir and E. Chaissaing, *J. Appl. Electrochem.* **26** (1996) 487.
16. M. Ebn Touhami, E. Chaissaing and M. Cherkaoui, *Electrochim. Acta* **43** (1998) 1721.
17. L.M. Abrantes and M.C. Oliveira, *Electrochim. Acta* **41** (1996) 1703.
18. N. Petrov, Y. Sverdlov and Y. Shacham-Diamand, *J. Electrochem. Soc.* **149** (2002) C187.
19. K.M. Gorbunova, M.V. Ivanov and V.P. Moiseev, *J. Electrochem. Soc.* **120** (1973) 613.
20. Z. Jusys, J. Liaukonis and A. Vaškelis, *J. Electroanal. Chem.* **325** (1992) 247.
21. I. Genutiene, J. Lenkaitiene, Z. Jusys and A. Luneckas, *J. Appl. Electrochem.* **26** (1996) 118.

22. W. Blum and G. Hogaboom, '*Principles of Electroplating and Electroforming (Electrotyping)*', 3rd edn. (McGraw-Hill, New York, 1949), p. 349.
23. F.A. Lowenheim, 'Electroplating', (McGraw-Hill, New York, 1978), p. 142.
24. A. Brenner, '*Electrodeposition of Alloys, Principles and Practices*', Vol. 2 (Academic Press, New York, 1963), p. 457.
25. L.M. Abrantes, M.C. Oliveira, J.P. Correia, A. Bewick and M. Kalaji, *J. Chem. Soc., Faraday Trans.* **93** (1997) 1119.
26. E.J. Podlaha and D. Landolt, *J. Electrochem. Soc.* **144** (1997) 1672.
27. I. Ohno, *Mater. Sci. Eng.* **A146** (1991) 33.
28. L.D. Burke and B.H. Lee, *J. Appl. Electrochem.* **22** (1992) 48.
29. R. Stevanovic, J. Stevanovic and A. Despic, *J. Appl. Electrochem.* **31** (2001) 855.
30. A.H. Gafin and S.W. Orchard, *J. Appl. Electrochem.* **22** (1992) 830.
31. T. Homma, I. Komatsu, A. Tamaki, H. Nakai and T. Osaka, *Electrochim. Acta* **47** (2001) 47.
32. C. Wagner and W. Traud, *Z. Elektrochem.* **44** (1938) 391.